since 1961

Baltica

BALTICA Volume 38 Number 2 December 2025: 113–129
https://doi.org/10.5200/baltica.2025.2.1

High-resolution geophysical and geochemical assessment for Cr-Ni deposit identification in ophiolitic complexes: the Arızlı case study (Afyon, Turkey)

Cihan Yalcin

Yalcin, C. 2025. High-resolution geophysical and geochemical assessment for Cr-Ni deposit identification in ophiolitic complexes: the Arızlı case study (Afyon, Turkey). *Baltica 38 (2)*, 113–129. Vilnius. ISSN 1648-858X.
Manuscript submitted 26 February 2025 / Accepted 9 September 2025 / Available online 10 October 2025

Abstract. The present study investigates the mineralization potential of the Arızlı ophiolitic complex in Afyon, Turkey, employing an integrated methodology that combines sophisticated geophysical and geochemical techniques. The area, characterized by ultramafic rock types and intricate structures, exhibits significant enrichment in chromium (Cr_2O_3, up to 49.51%) and nickel (Ni levels exceeding 2,000 ppm), particularly in serpentinized dunite regions. High-resolution drone-based magnetic surveys have detected anomalies indicative of ore-rich zones, with spatial data refined to resolutions of 50 m, 100 m, 150 m, and 250 m. Complementary IP/ERT profiling has identified chargeability and resistivity anomalies that align with the geochemical results. The geochemical investigation, performed using XRF, ICP-MS, and XRD, has confirmed these anomalies, revealing a complex mineralization framework mainly consisting of chromite, serpentine, and sulfide minerals, including pyrite and pentlandite. A comparative examination with global chromite-bearing ophiolites, including those in Oman and Greece, underscores the Arızlı region's correlation with economically significant deposits. The research highlights the influence of structural discontinuities, fault-induced hydrothermal modifications, and brecciation processes on the distribution of minerals. This research highlights the benefits of integrating geophysical and geochemical techniques for studying chromite and nickel in ophiolitic environments. The employed methodology may act as a reference framework for analogous studies in structurally intricate ultramafic terrains.

Keywords: *Arızlı ophiolitic complex; chromium and nickel mineralization; drone-based magnetic survey; induced polarization; geochemical analysis; ultramafic lithologies*

Cihan Yalcin (cihanyalcinjeo@gmail.com), https://orcid.org/0000-0002-0510-2992
SRG Engineering and Consultancy Ltd. Şti, Aydın, Türkiye

INTRODUCTION

Ophiolitic complexes are primary sources of strategic minerals globally, including chromite, nickel, and titanium. Their formation is linked to the emergence of mantle and oceanic crustal materials, which contribute to diverse mineralization processes (Leblanc, Nicolas 1992; Dilek, Furnes 2011; Robinson *et al*. 2015; Yang *et al*. 2021). In mineral-abundant areas, such as Turkey, these complexes have a significant economic value (Çiftçi *et al*. 2019). The ophiolitic complexes of western Anatolia are distinguished by their chromite deposits and nickel enrichment (Robertson 2002; Parlak *et al*. 2009).

Innovations in contemporary mineral exploration tools have expedited the mineral-finding process. Specifically, drone-based magnetic surveying and induced polarization (IP) techniques are notable for their capacity to provide high-resolution data and efficiently include extensive regions (Jackisch 2020; Park, Choi 2020; Jackisch *et al*. 2021). These techniques can be combined with electrical resistivity tomography (ERT), thereby enhancing our understanding of subsurface mineral distribution (Jackisch 2020; Ali *et al*. 2023; Yalçın, Karan 2024). Airborne magnetic data collection is crucial for identifying economically viable mineral resources, as it enables rapid data acquisition across extensive regions com-

pared to ground-based observations (Blakely 1996; Telford *et al*. 1990; Tobi *et al*. 2025).

The Arızlı area (Afyon, Turkey) has a considerable potential for essential minerals like chromite, nickel, and titanium. Nonetheless, prior investigations in this area have been confined to geological and geochemical assessments (Robertson 2002; Parlak *et al*. 2009; Çiftçi *et al*. 2019; Yalçın, Kaya 2025). This work seeks to address existing gaps in literature by integrating drone-based magnetic measurements, induced polarization, and geochemical analysis to ascertain the mineral distribution in the area.

Geochemical studies are essential for identifying the chemical fingerprints of mineralization processes. XRF and ICP-MS techniques enable a precise assessment of mineral chemical composition, and when combined with geophysical data, provide a comprehensive model of subsurface structures (Park, Choi 2020; Accomando *et al*. 2023). Integrating magnetic techniques with induced polarization (IP) has shown efficiency in the structural delineation of mineralization zones and a precise modelling of mineral deposits (Rashid *et al*. 2022; Sanusi *et al*. 2024; Fahad *et al*. 2025).

In recent years, notable advancements have been seen in the discovery and assessment of mineral resources by using drone-based magnetic surveying and induced polarization technologies (Blakely 1996; Park, Choi 2020; Tobi *et al*. 2025). Research conducted in New Zealand and Germany has shown the efficacy of these techniques in identifying various mineral resources (Rattenbury *et al*. 2016; Siemon *et al*. 2020; Cox *et al*. 2023). These methodologies remain inadequately used in ophiolitic complexes in Turkey, creating opportunities in regions such as Arızlı.

This research seeks to provide Turkey's mining industry with an innovative analytical framework and an extensive mapping of essential minerals in the Arızlı area. The study's results will enhance regional mineral exploration and illustrate the efficacy of novel techniques in this field.

GEOLOGICAL SETTING

The Arızlı ophiolitic complex is situated in the western branch of the Neotethyan suture zone in western Anatolia (Fig. 1a). This area constitutes a complicated tectonic zone established with the closure of the Neotethys Ocean and the subsequent obduction of oceanic lithosphere onto the Anatolian margin in the Late Cretaceous (Robertson 2002; Dilek, Furnes 2011).

Middle-Upper Triassic carbonates lie north and east of Arızlı, with Jurassic-Cretaceous limestones atop these formations. These strata are typically constrained by tectonic boundaries and are overlain by Upper Cretaceous ophiolite units to the south. The overlapping structures manifest as clips in specific locations. The development of these formations yields significant insights into the tectonic history of the area (Fig. 1b).

The primary geological units in the region comprise the ophiolitic mélange series, which includes peridotite, dunite, serpentinite, diabase, and basalt. These rocks display the east-west orientation, facilitating the production of minerals, including chromium, nickel, and titanium. Serpentinization and hydrothermal alteration processes are significant factors in enriching these minerals (Çiftçi *et al*. 2019).

Ophiolitic rocks from the Upper Cretaceous period characterize the Arızlı region. This unit consists of rocks such as serpentinite, dunite, gabbro, and basalt, and is typically subject to deformation and modification (Fig. 2). The ophiolitic series commonly exhibits basal lithologies, characterized by notable enrichments in chromium, nickel, gold, and titanium in these regions. The serpentinization in the area resulted from the interaction of ultramafic rocks with hydrothermal fluids, considerably contributing to mineralization processes.

Dunite concentrations are very significant for chromite mineralization. The fault zones in these units influenced the brecciation and weathering apparent in the area. A right-lateral strike-slip fault traverses the region and significantly contributes to mineralization by facilitating hydrothermal alteration processes. This fault also triggered the formation of additional faults in the area and facilitated the development of alteration zones along structural discontinuities.

The southern part of the region contains Upper Cretaceous limestones and Lower-Upper Oligocene red gravestones. These units are located along the thrust line of the ophiolitic series and lack any economically significant mineralization. The ophiolitic mélange is intersected in certain areas by strike-slip faults, which govern the settlement.

The geological formations in the Arızlı region are situated within a structural framework governed by strike-slip and dip-slip faults. These faults influenced both the deformation of the rocks and the alteration processes (Fig. 2). The limestone-antiolite mélange is recognized as a significant structural discontinuity in the region. The deformation and brecciation along this discontinuity have significantly contributed to mineralization.

Alteration and brecciation, noted in the contact zones of the ophiolitic series, have modified the internal structure and physical properties of the ultramafic rocks. Hydrothermal circulations along the faults altered the rocks' chemical characteristics and enhanced their mineralization potential. Serpentinites are mainly distinguished by their low magnetic sus-

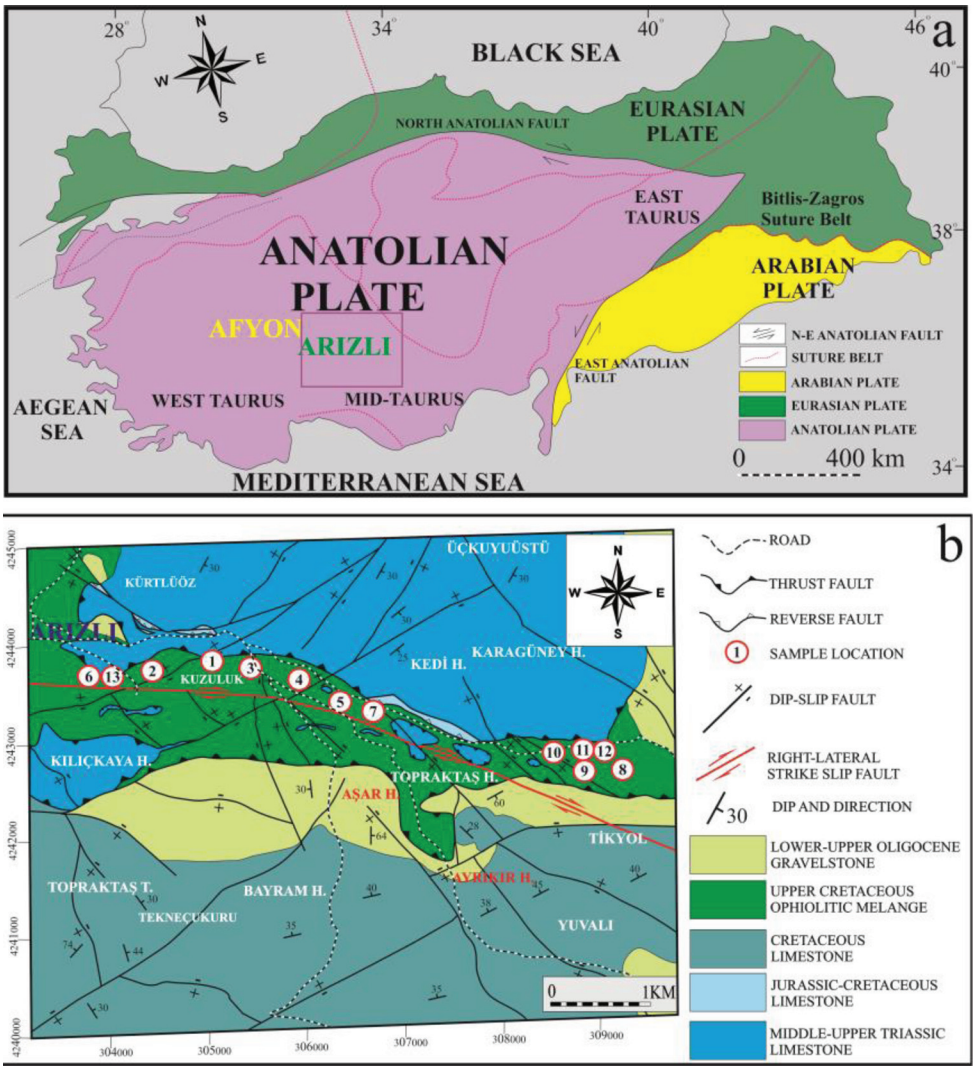

Fig. 1 (a) Tectonic location of the study area (modified from Işık 2016) and (b) comprehensive geological map of the research region (adapted from MTA L25 B4 sheet at a scale of 1:25,000)

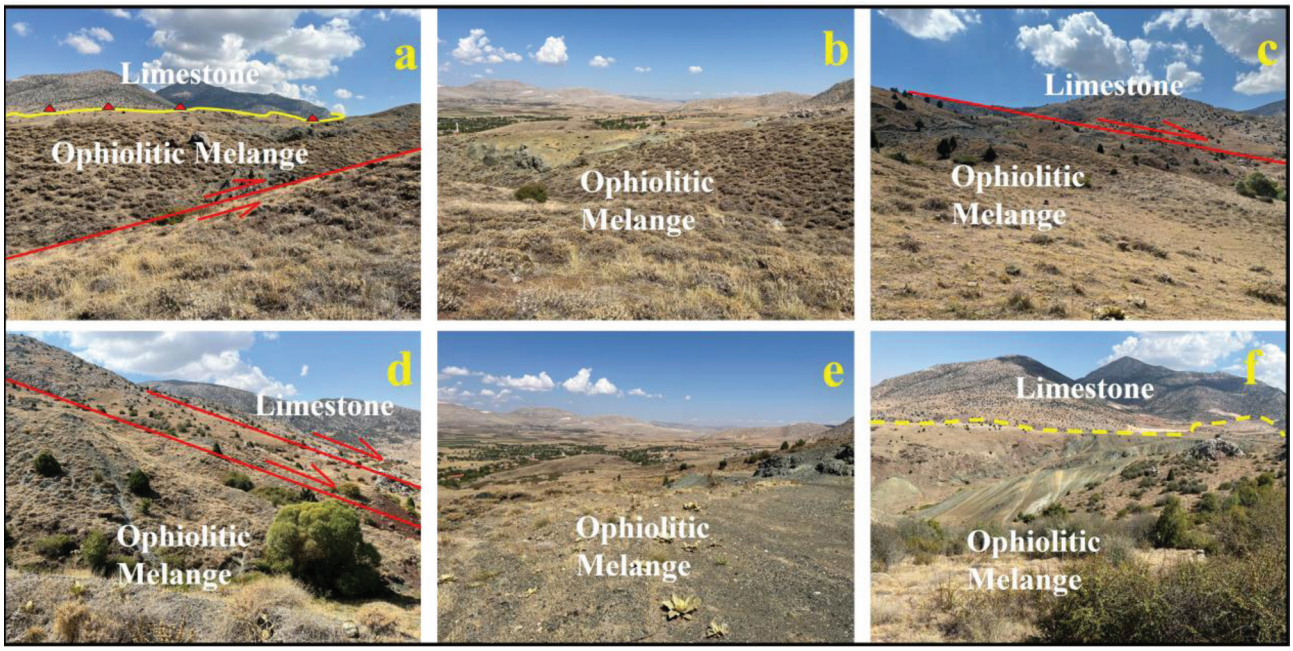

Fig. 2 A field perspective illustrating the contact interactions between ophiolitic units (dunite, serpentinite, and basalt) and limestone formations (a–f)

ceptibility and elevated resistivity values (Telford *et al*. 1990).

The region's most notable structural feature is the east-west-oriented right-lateral strike-slip fault (Fig. 1). This fault has significantly influenced the weathering and alteration of ultramafic rocks in the region, resulting in the brecciation of minerals and their transformation into economically valuable sources of enrichment. Serpentinization and hydrothermal circulation processes have been documented along fault zones, influencing the subsurface distribution of minerals, including chromium, nickel, and titanium. The mafic lithologies of the ophiolitic series in the research area were more extensive, indicating a significant potential for mineralization.

MINERALIZATION

Chromite and nickel mineralization in the Arızlı region is concentrated in the ultramafic levels of the ophiolitic mélange. This mineralization signifies commercially essential deposits, particularly in dunite and serpentinite lithologies. Field observations and laboratory analyses yield critical insights into the mineralization's geometry, structural linkages, and mineralogical characteristics (Figs 3 and 4).

Mineralization is seen in veins of 1–5 meters in width and broader breccia zones (Figs 3 and 4). Breccias are discovered in places of intense mineralization because of the influence of the right-directional strike-slip fault. This fault influenced the weathering and redistribution of chromite and nickel minerals, promoting the accumulation of sulfide minerals, including pyrite and pentlandite, within brecciated and fractured textures. Serpentinization and hydrothermal alteration are frequently observed in mineralization zones (Fig. 3). Alteration zones resulted in the localized enrichment of oxide minerals, namely hematite and limonite.

Although chromite mineralization is generally massive, a disseminated texture is also observed in some zones. Extensive chromite veins are localized in dunite units, and these minerals often consist of euhedral crystals. In brecciated zones, chromite minerals have more aberrant textures. This indicates that mineralization was reconfigured and distorted due to the impacts of faulting.

MICROSCOPIC ANALYSES AND MINERALOGICAL COMPOSITION

Petrographic investigations were conducted on thin sections by using both plane-polarized light (PPL) and cross-polarized light (XPL) microscopy to determine the mineralogical composition and microstructural characteristics of the chromite-bearing samples. The samples predominantly consist of serpentine (serp), calcite (cal), and opaque minerals (opq), as illustrated in Fig. 5. The predominant opaque phases consist of chromite and minor sulfides, including pyrite. Chromite grains frequently manifest as euhedral to subhedral crystals; nevertheless, deformation characteristics, including fracturing and replacement textures, are also apparent. These fissures presumably functioned as channels for hydrothermal

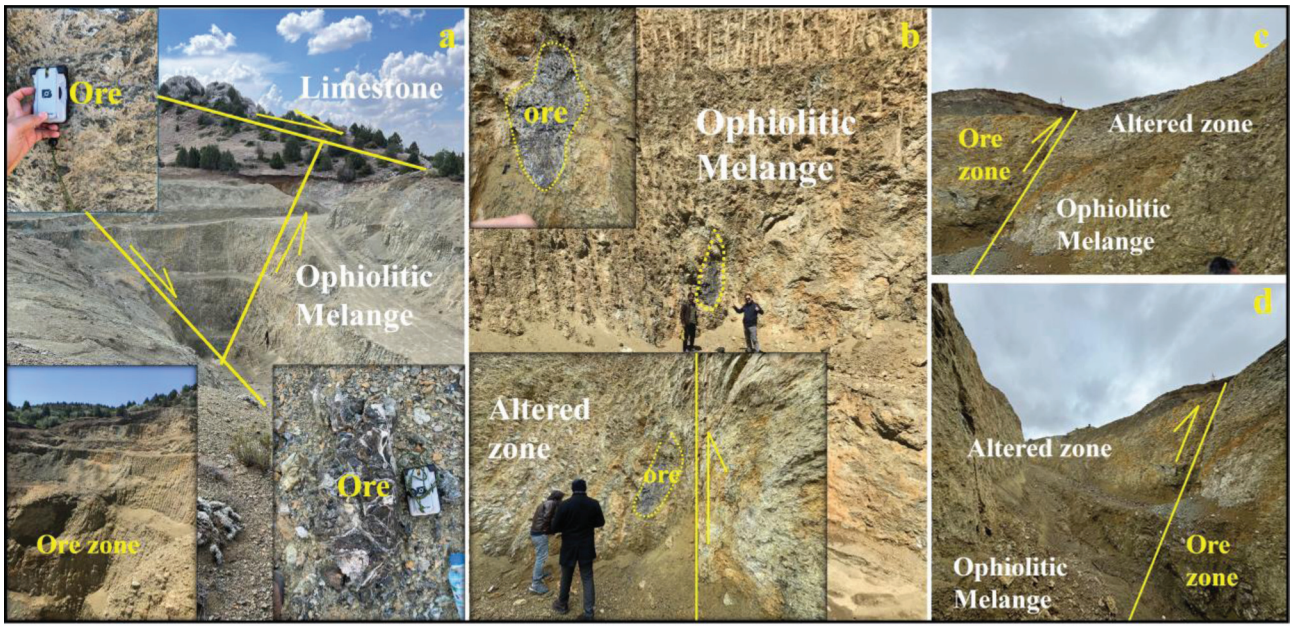

Fig. 3 Images of mining zones and geological formations within the research region. The photos illustrate the morphological and mineralogical correlations of the surface ore zones: (a) ore zones linked to faults and ophiolitic mélange, (b) surface manifestation of the ophiolitic mélange and altered regions, (c) alteration zone and its correlation with ore zones, (d) in-depth examination of a particular ore zone

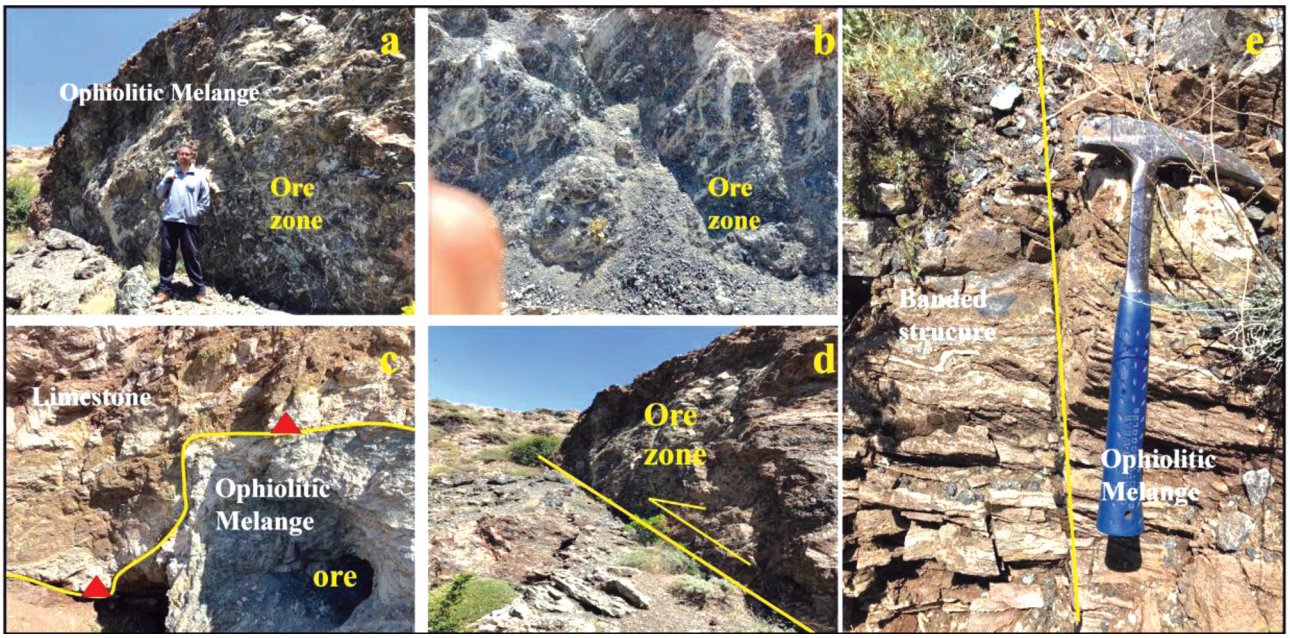

Fig. 4 Images of mining zones and geological formations within the research region: (a–b) ore zone, (c) thrust contact between limestone and ore zone, (d) fault in ore zone, (e) banded structure in ophiolitic melange

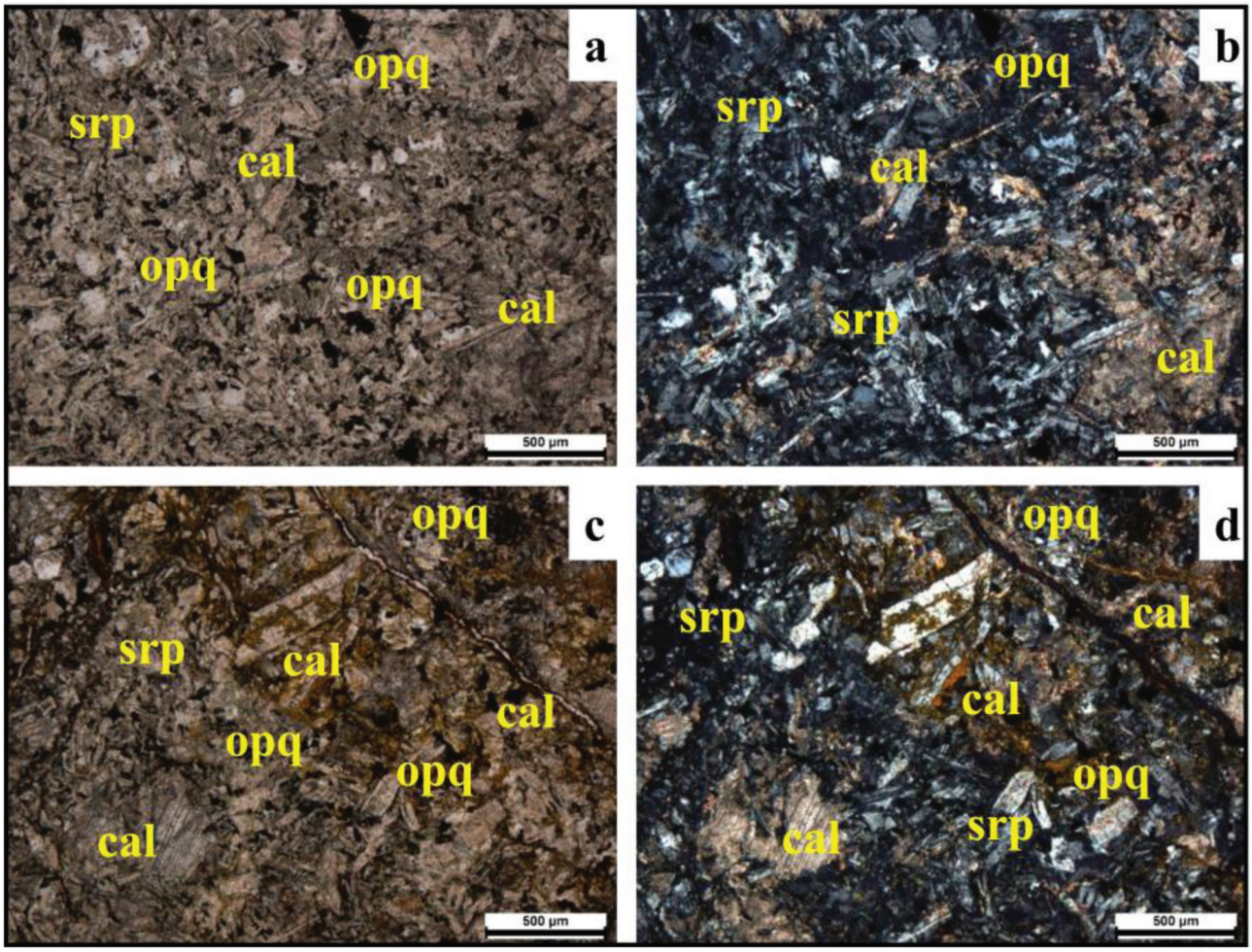

Fig. 5 Exemplary photomicrographs of thin sections from chromite-bearing serpentinites observed under plane-polarized light (a, c) and cross-polarized light (b, d). The microtextures indicate the prevalence of serpentine (serp), calcite (cal), and opaque minerals (opq), aligning with hydrothermal alteration (mineral abbreviations after Whitney, Evans 2010)

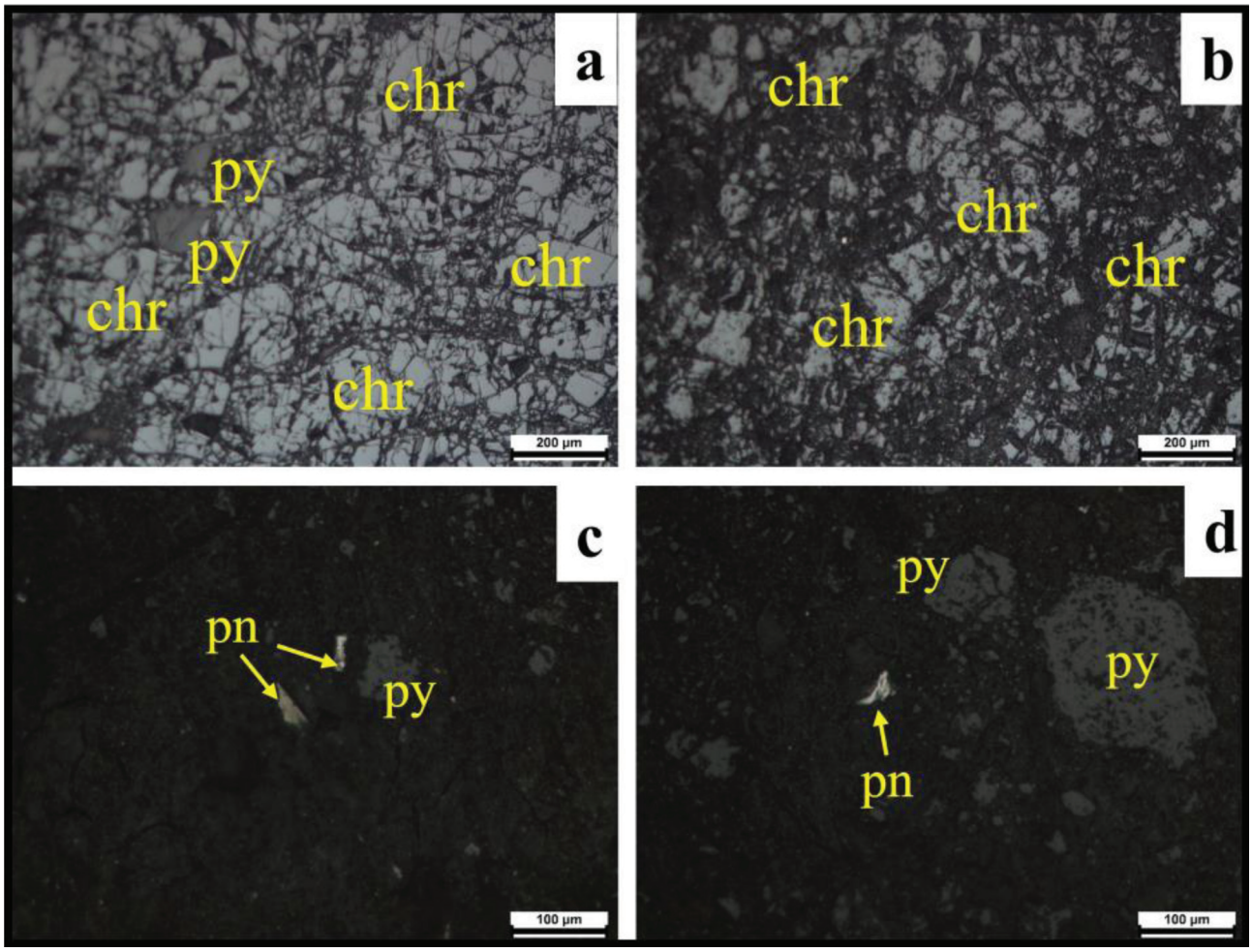

Fig. 6 Photomicrographs of polished sections showing ore minerals in chromite-bearing serpentinites: (a, b) brecciated chromite (chr) grains with interstitial pyrite (py), (c, d) pentlandite (pn) co-occurring with pyrite (py), suggesting late-stage sulfide mineralization along microfractures (mineral abbreviations after Whitney, Evans 2010)

fluids, facilitating metasomatism and recrystallization. The photomicrographs demonstrate significant serpentinization and calcite veining, suggesting post-magmatic fluid action. All mineral abbreviations utilized adhere to the standard established by Whitney, Evans (2010).

Reflected light microscopy was used to examine the polished sections of chromite-bearing samples to characterize ore mineral assemblages and textures. The main ore minerals identified were chromite (chr), pyrite (py), and pentlandite (pn), as illustrated in Fig. 6. Chromite typically appears as brecciated and fractured grains, often surrounded by pyrite along grain boundaries and in interstitial spaces (Fig. 6a, b). In many instances, pentlandite occurs together with pyrite within microfractures and late-stage veins, indicating a secondary phase of sulfide mineralization likely associated with hydrothermal processes (Figs 6c and 6d). These textures strongly suggest that deformation and fluid activity along fault zones controlled the remobilization and redistribution of sulfides.

The X-ray difrfraction (XRD) investigation revealed the presence of lizardite and chlorite minerals, with chromite, serpentine, pyrite, and pentlandite minerals in the ore samples collected from the location (Fig. 7). These minerals exhibit the mineralogical evidence of serpentinization and hydrothermal alteration activities. The unique mineralogical and textural properties of the chromite ore suggest that the mineralization in the area is associated with the basal lithologies of ophiolitic rocks.

The analyses have comprehensively elucidated the structural and mineralogical attributes of mineralization in the Arızlı region. Breccia textures, alteration zones, and fault influences are pivotal in the distribution of chromite and nickel minerals in the area. The microscopic and XRD data provide a robust foundation for evaluating the economic viability of this deposit and determining the region's mining significance. In conjunction with continuous geochemical analysis, this data will facilitate the advancement of novel methodologies for mineral exploration.

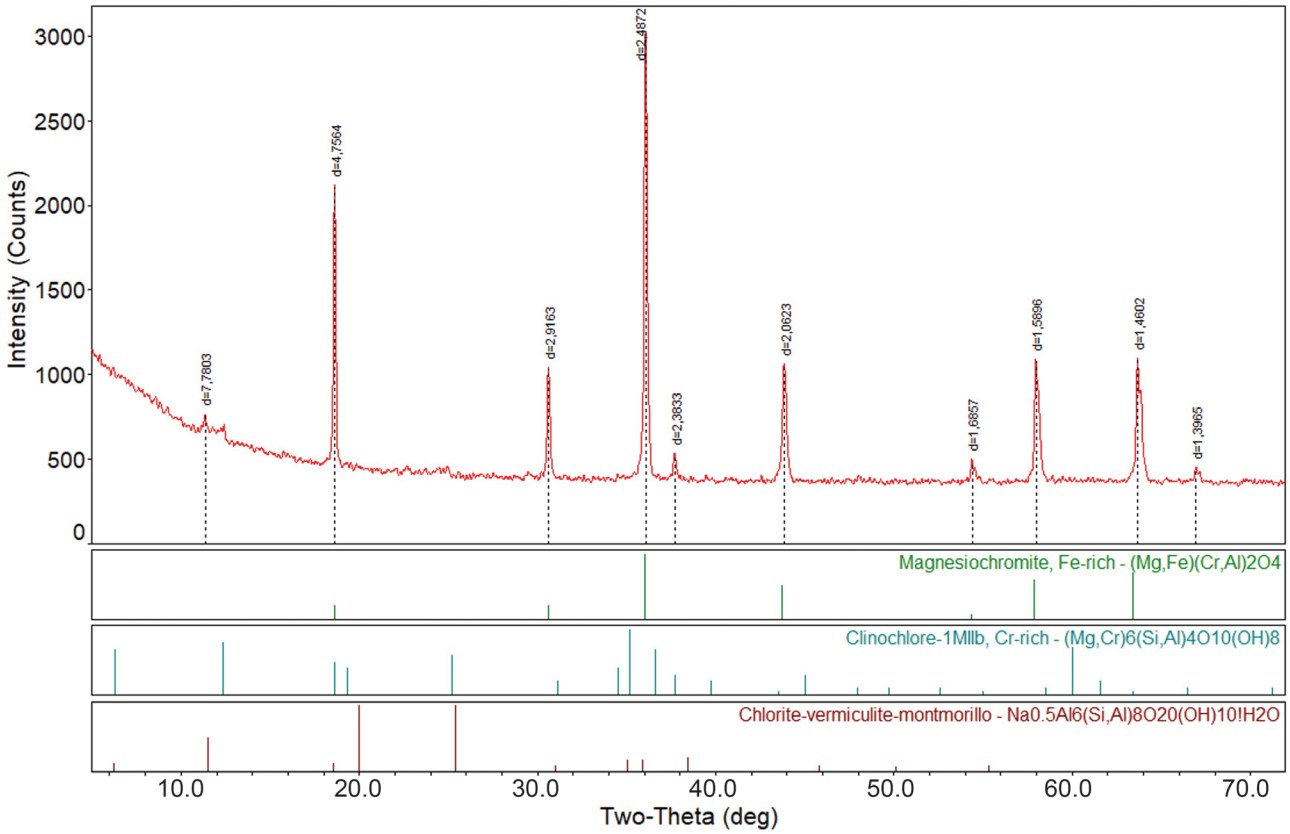

Fig. 7 XRD study findings emphasize the crystalline structures of several minerals. Diffractograms of the samples revealed the presence of principal mineral phases, including calcite, serpentine, and chromite

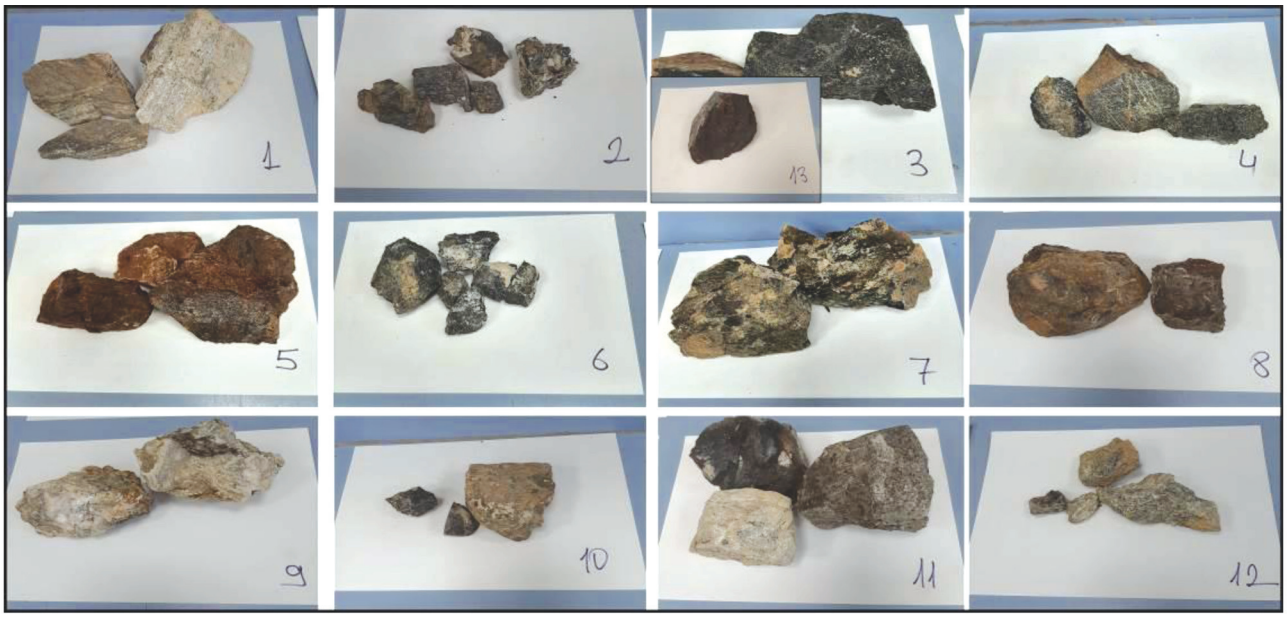

Fig. 8 Geological specimens obtained from the research area

SAMPLING AND ANALYTICAL METHODS

The research involved collecting 13 samples from a specific location to examine lithological diversity and identify regions with a significant mineralization potential (Fig. 8). The materials were carefully processed (Fig. 1) and comprehensively investigated at the Geochemistry Research Laboratory of Istanbul Technical University. The samples were ground using a RETSCH RS-200 grinder, and geochemical studies were conducted using X-ray fluorescence spectrometry (XRF) and inductively coupled plasma-mass spectrometry (ICP-MS) devices. For ICP-MS analysis, each sample was entirely dissolved in Te-

flon containers utilizing a mixture of 37% hydrochloric acid, 65% nitric acid, and 38–40% hydrofluoric acid (HF). The surplus HF acid was eliminated by adding a 5% H_3BO_3 solution. The produced solutions were transferred to 50 mL balloon flasks containing distilled water, resulting in clear solutions. An identical procedure was used to create the blank solution, which served as a reference.

The X-ray diffraction (XRD) investigations were conducted using a Bruker D8 Advance model of equipment, employing Cu Kα radiation and X'Pert HighScore Plus v. 3.0 software to identify mineral phases and semi-quantitatively assess mineral species in the samples.

The Geometrics G-882 magnetometer, commonly utilized in marine and terrestrial contexts, was modified for aerial deployment by affixing it beneath a drone for this survey. The drone operated at a consistent speed at an altitude of 50 metres, collecting magnetic field data along flight lines spaced 50 meters apart across a 12 km² research area. The aircraft trajectories were designed to cover the whole study region. The collected raw magnetic data was processed with the Oasis Montaj software. Initially, the reduction to pole (RTP) was applied to the data to eliminate local magnetic field effects, followed by low-frequency filtering to reveal regional anomalies. The resultant magnetic anomalies facilitated a detailed mapping of the distribution of magnetic materials beneath the location.

Electrical resistivity tomography (ERT) and induced polarization (IP) measurements were conducted using the ABEM Terrameter LS instrument (Fig. 9). ERT measurements along ten profiles in the research area (Fig. 10) produced 2D resistivity sections that comprehensively depict the underlying structures. Resistivity cross sections were calibrated with a minimum threshold of 9.8 Ohm-m (blue) and a maximum threshold of 447 Ohm-m (red). Low resistivity levels typically signify zones with changed properties and high clay content, whereas high resistivity values indicate mineralized zones. IP measurements were used to evaluate chargeability values, revealing abnormalities of 1% and 5%. The IP sections were analyzed using numerical data rather than colour coding, facilitating a more precise evaluation of the chargeability anomalies.

The dependability of the data acquired from aerial magnetic and IP/ERT measurements was assessed by computing root mean square (RMS) error rates. The

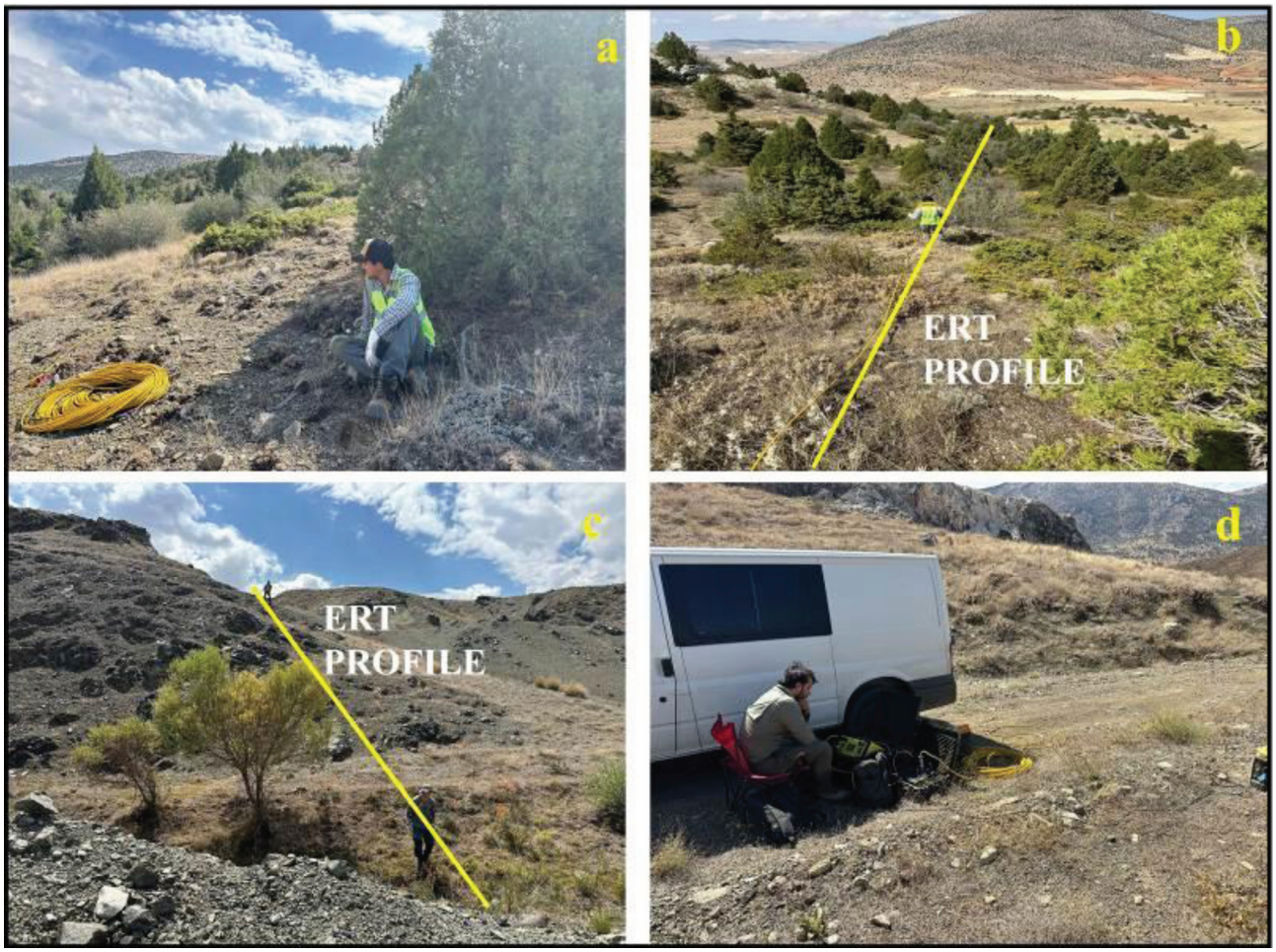

Fig. 9 Equipment for IP and ERT measurements and the methodologies employed during the field investigation (a–d)

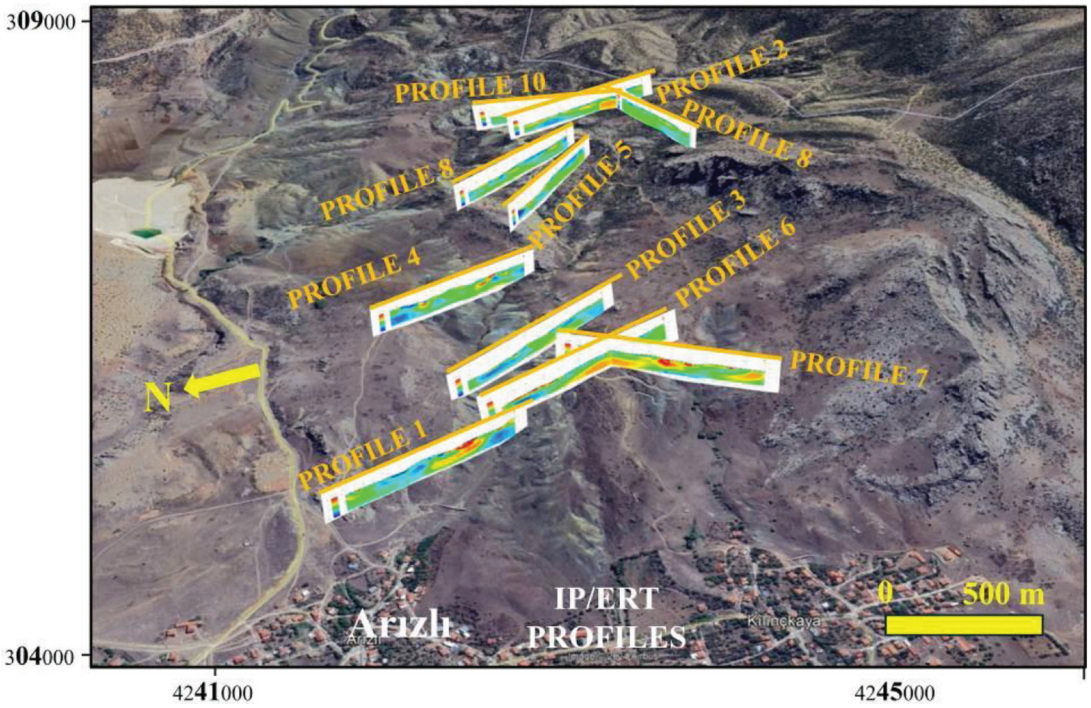

Fig. 10 The map indicating the locations of IP and ERT profiles within the research area

RMS error rate was calculated to be 2.3% for the resistivity data and 3.1% for the induced polarization data. The RMS calculations validated the precision of the instrument calibration and the dependability of the field measurements. The error rates strongly corroborate the dependability of the data obtained. Additionally, spontaneous potential (SP) measurements were employed as an auxiliary method to support the determination of structural features, including fault zones, formation boundaries, and surface water distribution. The SP data supplied essential information for identifying alteration zones and structural discontinuities in the research area.

GEOCHEMISTRY

The geochemical investigations of rock samples from the Arızlı region yield extensive data for assessing the mineralization potential in the area. The principal oxide results derived from the XRF approach unambiguously indicate the ultramafic nature of the ophiolitic mélange units (Table 1). The notably elevated Cr_2O_3 concentrations in samples ARIZLI-6 (41.66% Cr_2O_3) and ARIZLI-13 (49.51% Cr_2O_3) suggest chromite mineralization with commercial viability. Furthermore, the elevated levels of Fe_2O_3 (ranging from 16.29% to 18.57%) and MgO (spanning from 10.42% to 37.71%) substantiate the ultramafic origin of the rocks. The LOI (loss on ignition) values, particularly in sample ARIZLI-9 (35.23%), indicate significant hydrothermal alteration and carbonatization processes.

The trace element investigation by ICP-MS provided a more detailed information on the geochemical properties of the chromatic zones. Table 2 illustrates that Ni, Co, and V concentrations provide distinct evidence of ultramafic mineralization. For example, samples ARIZLI-6 (1002 ppm Ni, 153 ppm Co) and ARIZLI-13 (1566 ppm Ni, 132 ppm Co) suggest chromite- and nickel-enriched units. The presence of elements such as Zn, Sr, and Zr signifies the complexity of the mineralization processes in the region. The concentration of vanadium (V) exhibited notable enrichment, particularly in samples ARIZLI-6 (758 ppm) and ARIZLI-13 (682 ppm). Geochemical investigations unequivocally indicate that the mineralization in the region presents substantial potential. The elevated Cr_2O_3 and Ni concentrations, particularly inside the chromitic zones, signify the existence of economically viable deposits. These findings, together with field observations and geophysical data, facilitate the assessment of the mineral potential in the research region.

RESULTS AND ASSESSMENT OF GEOPHYSICAL MEASUREMENTS

Comprehensive geophysical measurements were conducted at the Arızlı location as part of the investigation. These measurements utilized aircraft magnetic data collecting and IP/ERT (induced polarization and electrical resistivity tomography) techniques. Figure 10 illustrates the trajectories of the IP/ERT profiles, while Fig. 11 presents the maps of the aerial magnetic data at the depths of 50 m, 100 m, 150 m, and 250 m. Figure 13 illustrates the outcomes derived from the IP and ERT methodologies.

Table 1 Major oxide analyses of samples from the Arızlı Region (XRF results)

XRF	Na_2O	MgO	Al_2O_3	SiO_2	P_2O_5	K_2O	CaO	TiO_2	MnO	Fe_2O_3	Cr_2O_3	SO_3	LOI
SAMPLE	%	%	%	%	%	%	%	%	%	%	%	%	%
ARIZLI 1	0.52	2.67	5.77	47.88	0.15	2.46	24.57	0.71	0.19	4.82	0.02	0.03	10.12
ARIZLI 2	< 0.01	27.09	1.40	31.64	< 0.01	0.03	13,02	0.06	0.14	9.68	0.35	0.02	16.31
ARIZLI 3	1.47	10.42	10.22	37.62	0.78	0.85	14.41	**3.67**	0.22	18.57	0.08	< 0.01	1.52
ARIZLI 4	1.64	10.49	9.83	39.95	0.62	0.89	14.46	**2.35**	0.32	17.37	0.12	< 0.01	1.81
ARIZLI 5	0.05	1.81	1.45	76.35	0.06	0.19	9.40	0.09	0.70	4.02	0.01	0.01	5.80
ARIZLI 6	< 0.01	16.73	9.44	9.82	< 0.01	< 0.01	2.92	0.14	0.15	16.29	**41.66**	< 0.01	2.58
ARIZLI 7	0.64	9.49	11.26	36.17	0.52	0.27	18.13	**2.88**	0.20	14.53	0.29	< 0.01	5.49
ARIZLI 8	4.03	5.56	11.46	39.38	0.16	0.26	13.56	**1.78**	0.26	12.88	0.03	0.02	10.52
ARIZLI 9	0.10	0.85	1.23	11.92	< 0.01	0.25	49.43	0,08	0.18	0.63	0.03	0.03	35.23
ARIZLI 10	< 0.01	34.28	0.29	38.54	< 0.01	< 0.01	1.14	0.16	< 0.01	10.82	0.34	0.01	14.09
ARIZLI 11	< 0.01	37.71	0.17	34.73	< 0.01	< 0.01	0.39	<0.01	0.14	9.87	0.39	< 0.01	16.29
ARIZLI 12	< 0.01	35.34	0.24	35.34	< 0.01	< 0.01	5.65	0.01	0.14	7.31	0.36	0.02	15.37
ARIZLI 13	< 0.01	15.24	11.83	3.84	< 0.01	< 0.01	1.11	0.19	0.15	16.18	**49.51**	< 0.01	1.64

Table 2 Trace element analyses of samples from the Arızlı Region (ICP-MS results)

ICP/MS	Sc	V	Co	Ni	Cu	Zn	As	Sr	Zr	Nb	Mo	Ba	Pb
SAMPLE	ppm	ppm	ppm	ppm	ppm	ppm	ppm	ppm	ppm	ppm	ppm	ppm	ppm
ARIZLI 1	7.00	61.00	16.00	51.00	13.00	46.00	16.00	213.00	77.00	13.00	1.00	258.00	< 1
ARIZLI 2	12.00	69.00	94.00	**1827,00**	10.00	34.00	9.00	73.00	16.00	1.00	2.00	35.00	< 1
ARIZLI 3	30.00	260.00	65.00	350.00	197.00	127.00	10.00	165.00	247.00	44.00	1.00	86.00	< 1
ARIZLI 4	35.00	209.00	73.00	439.00	38.00	170.00	12.00	163.00	147.00	31.00	1.00	50.00	< 1
ARIZLI 5	5.00	48.00	35.00	30.00	80.00	49.00	23.00	39.00	29.00	4.00	2.00	32.00	< 1
ARIZLI 6	< 1	758.00	153.00	**1002,00**	17.00	383.00		51.00	14.00	< 1	1.00	17.00	< 1
ARIZLI 7	29.00	245.00	55.00	235.00	72.00	97.00	12.00	152.00	193.00	39.00	1.00	35.00	< 1
ARIZLI 8	38.00	358.00	24.00	42.00	25.00	81.00	17.00	156.00	86.00	5.00	1.00	58.00	< 1
ARIZLI 9	1,00	42.00	1.00	28.00	8.00	19.00	10.00	148.00	24.00	2.00	6.00	< 1	< 1
ARIZLI 10	5.00	12.00	**127.00**	**2145,00**	1.00	39.00	11.00	22.00	13.00	2.00	1.00	14,00	< 1
ARIZLI 11	7.00	18.00	**113.00**	**1789,00**	< 1	36.00	9.00	6.00	12.00	1.00	1.00	7,00	< 1
ARIZLI 12	10.00	26.00	**117.00**	**1588,00**	4.00	23.00	16.00	103.00	14.00	2.00	2.00	18.00	< 1
ARIZLI 13	< 1	682.00	**132.00**	**1566,00**	17.00	299.00	10.00	7.00	14.00	1.00	2.00	21.00	< 1

Aerial magnetic measurements

Magnetic measurements were acquired via an uncrewed aerial vehicle (UAV). Figure 11 illustrates the spread of magnetic anomalies across various depths. The map at a depth of 50 m (Fig. 11c) reveals anomalies close to the surface, but the maps at the depths of 100 m (Fig. 11d), 150 m (Fig. 11e), and 250 m (Fig. 11f) illustrate the magnetic properties of subsurface structures. The findings reveal a significant magnetic anomaly in the region, which is believed to be linked to chromite and nickel enrichments.

Airborne magnetic maps indicate that the anomalies are predominantly aligned in the northeast-southwest orientation. This illustrates the structural regulation of the ophiolitic mélange in the research area, as well as fault zones potentially linked to mineralization.

IP/ERT measurements

Figure 12 presents the IP and ERT results, offering a comprehensive analysis of the electrical characteristics of the site's subsurface structures. Ten profiles were acquired, and resistivity and IP sections were generated based on these profiles. Resistivity data were normalized between 9.8 Ω and 447 Ω, with low resistivity values represented in blue, and high resistivity values in red. Low resistivity readings are typically associated with altered zones and possibly mineralized regions.

The IP measurements indicated elevated chargeability values, suggesting the presence of metallic minerals. These findings offer significant evidence for mineralization zones in the field. The anomalies detected in the IP sections confirm the presence of mineralized zones indicative of chromite and nickel enrichments.

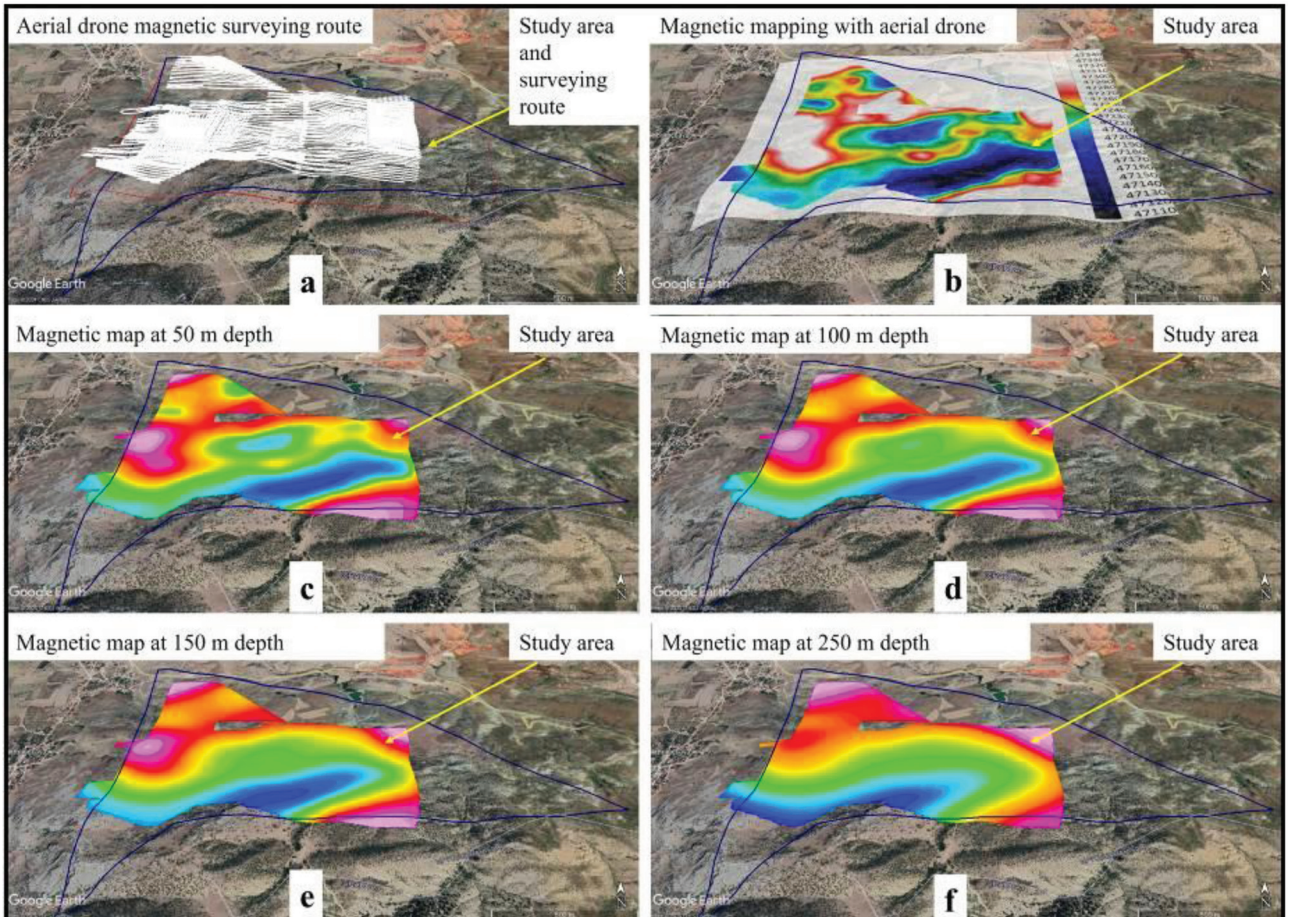

Fig. 11 Results of the magnetic survey acquired by drone measurements: (a) survey paths for drone-operated magnetic measurements across the research region, (b) magnetic cartography obtained from aerial data, (c–f) three-dimensional representation of magnetic anomalies at different depths (50 m, 100 m, 150 m, and 250 m)

Error rates were calculated to assess the dependability of the geophysical data obtained. During the processing of airborne magnetic measurements, corner deviations and magnetic noise were eliminated, thereby enhancing measurement accuracy. In modelling IP/ERT data, the root mean square (RMS) error rate was maintained below 5%, signifying the reliability of the results.

Analysis of spontaneous potential (SP) data

The SP data was a supplementary technique for identifying fault zones and surface water dynamics. Measurements revealed substantial negative and positive anomalies in the studied area. Negative SP anomalies were typically associated with altered zones, whereas positive anomalies were correlated with surface water flow.

The geophysical survey results have effectively shown structural and altered zones potentially linked to chromite and nickel enrichments in the studied region. The IP and ERT measurements, along with the magnetic anomalies, offer compelling evidence of the area's mineralization potential. Specifically, regions exhibiting elevated chargeability in IP data have been designated priority targets for comprehensive mineral exploitation.

DISCUSSION

This study's integration of geophysical and geochemical methodologies has yielded significant insights into the mineralization potential of the Arızlı region, which is notable for its ophiolitic mélange and substantial mineral resources, including chromite and nickel. The comprehensive methodology utilized herein, encompassing drone-based magnetic surveys, IP/ERT profiling, and sophisticated geochemical analysis, illustrates both the benefits and difficulties of these techniques in exploring analogous deposits worldwide.

Analysis of international case studies

Global ophiolitic complexes, including those in Oman (Ahmed, Arai 2003), the Balkans (Kapsiotis 2014), and New Caledonia (Maurizot *et al*. 2020; Wells *et al*. 2022), have repeatedly exhibited substantial potential for the occurrence of chromite, nickel,

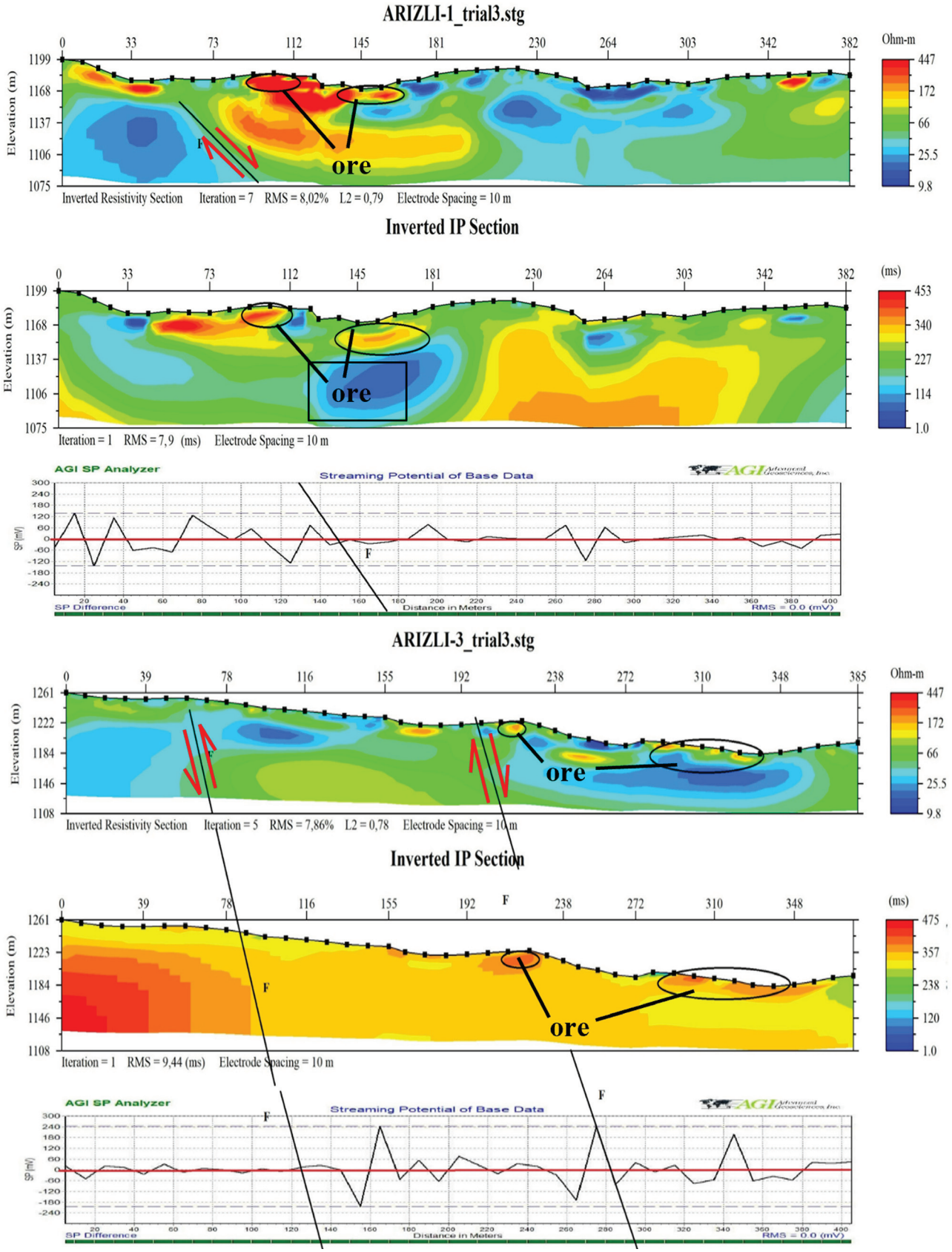

Fig. 12 Results and profiles of the IP/ERT survey. Sections of resistivity and induced polarization across several profiles in the studied area. Red and blue denote low and high resistivity zones, respectively, indicating the locations of ore deposits. The profiles highlight the correlation among faults, alteration zones, and mineralization

and associated minerals. The results from Arızlı align with these international observations, particularly in terms of the correlation between chromite mineralization and serpentinized ultramafic rocks. Eskandari *et al*. (2023) demonstrated that high-resolution drone-based magnetic surveys can accurately identify deep-seated mineralized formations, a finding similar to those in the Arızlı region.

Moreover, Turkey's chromite deposits, especially inside the Tethyan ophiolitic band (Çiftçi *et al*. 2019), exhibit significant parallels with the discoveries in Arızlı, particularly regarding structural restrictions and the occurrence of brecciated ore zones. The present work validates these findings by highlighting the significance of fault zones in promoting hydrothermal modifications and ensuing mineral enrichment, as documented in research from the Philippines (Dossey 2023) and Papua New Guinea (Smith *et al*. 2023).

Regional tectonic context and structural framework

The Arızlı ophiolitic complex is located within the extensive tectonic structure of the Neotethyan suture zone in western Anatolia, which documents the closing of the Neotethys Ocean and ensuing continental collision episodes during the Late Cretaceous (Robertson 2002; Dilek, Furnes 2011). The area is characterized by the presence of ultramafic units, including harzburgite, dunite, and serpentinized peridotite, which are frequently linked to thrusting and obduction at the continental edge. The Arızlı region exemplifies a tectonic mélange environment, characterized by significant deformation and brecciation along east-west-oriented right-lateral strike-slip faults, which played a pivotal role in concentrating hydrothermal alteration and chromitite mineralization.

The structural components indicate a post-subduction tectonic regime characterized by lithospheric thinning, slab break-off, and strike-slip faulting, which enabled mantle upwelling and subsequent magmatic activity. The placement of chromite-rich dunites and subsequent serpentinization presumably transpired along steep, structurally regulated zones, which currently serve as favoured pathways for fluid circulation and mineral concentration. This view corresponds with models suggested for analogous ophiolitic complexes in the Eastern Mediterranean and southern Tethyan regions (Parlak *et al*. 2009; Kapsiotis 2014).

Assessment of geophysical methodologies

Drone-based magnetic surveys have demonstrated significant utility in identifying underlying anomalies in extensive and challenging landscapes. Drone-based systems offer superior spatial resolution and expedite data collection relative to traditional ground-based methods, as demonstrated by recent research conducted by Park and Choi (2020), Jackisch *et al*. (2021), and Li *et al*. (2024). This study also encountered constraints, including vulnerability to ambient noise and the need for sophisticated data processing algorithms, as noted by Dadrass *et al*. (2024).

The IP/ERT profiling was crucial in detecting resistivity and chargeability abnormalities, which signified mineralized zones (Alshareef *et al*. 2025). The results align with those of the Yukon chromite deposits in Canada (Cross, Peterson 2023) and the Bushveld Complex in South Africa (Kruger 2021; Sihoyiya 2023), where IP/ERT profiling has been successfully employed. This work further highlights the challenges of scaling IP data to accurately represent more complex systems, echoing the concerns expressed by Davidenko *et al*. (2023).

The computed RMS errors of under 5% confirm the dependability (Harris, Grunsky 2015) of the IP/ERT data gathered in Arızlı. The accuracy aligns with studies conducted in Oman and the Philippines (Arai 1992; Ahmed, Arai 2003; Tupaz *et al*. 2020), which found analogous error margins, underscoring the robustness of the applied technique (Lelièvre, Farquharson 2016; Harris, Grunsky 2015).

Geochemical insights and global comparisons

The geochemical results from XRF, ICP-MS, and XRD examinations characterize the area's principal oxides, trace elements, and mineral phases. The elevated Cr_2O_3 content (up to 49.51%) and substantial Ni concentrations (> 2.000 ppm) found in the Arızlı samples position the location among the economically important chromite and nickel resources worldwide. Similar geochemical signatures have been reported in the Oman ophiolites (Arai *et al*. 2004) and the Pindos ophiolites in Greece (Zhou *et al*. 1996; Kapsiotis 2013, 2014, 2016; Zaccarini *et al*. 2024).

Additionally, the Cr/Fe ratios in the Arızlı chromites correspond with those documented from the Vourinos chromite deposits in Greece (Smith *et al*. 2024) and the Sukinda belt in India (Arasada *et al*. 2020; Mishra *et al*. 2022), hence reinforcing the economic potential of these deposits. This work successfully demonstrates the association between geochemical anomalies and geophysical data, a relationship previously observed in other mineralized belts, including the Abitibi greenstone belt in Canada (Mokhtari *et al*. 2025).

While rare earth element (REE) analysis was not performed in this phase of the study, subsequent research will incorporate REE and isotopic investigations to more accurately delineate the mantle source characteristics and assess potential metasomatic overprints.

Benefits and drawbacks of methodologies

The integrative technique employed in this study provides a multifaceted understanding of the subsurface geology. Drone-based magnetic surveys accurately defined extensive structural features, whilst IP/ERT profiling provided depth-specific resolution to the mineralized zones (Moezzi Nasab *et al*. 2023). The geochemical analyses enhanced these methods by confirming the mineralogical composition and elemental distribution.

Nevertheless, certain limits were identified. Drone-based magnetic surveys provided high-resolution data; nonetheless, their efficacy diminished in regions characterized by dense vegetation and steep topography, as noted by Efrem *et al*. (2024). Likewise, IP/ERT profiling encountered difficulties in areas with significant resistivity differences, which could obscure minor anomalies, a shortcoming identified in research by Li *et al*. (2023).

Consequences for subsequent exploration

The results from the Arızlı region highlight the efficacy of integrating contemporary geophysical and geochemical techniques for mineral prospecting. Integrating drone-based surveys with IP/ERT profiling constitutes a substantial development in locating deep-seated ore bodies, as notably highlighted in recent research (Jackisch 2020; Jackisch *et al*. 2021). Subsequent research may benefit from integrating supplementary techniques, such as magnetotellurics and 3D inversion modeling, which have demonstrated efficacy in alternative ophiolitic environments (Kruger 2021; Sihoyiya 2023).

Moreover, the data obtained from Arızlı can be a benchmark for investigating analogous deposits in other regions of Turkey and worldwide. The approaches and results provided here provide a comprehensive framework for appraising mineral potential in structurally complex terrains, particularly those associated with ophiolitic phases.

The investigation of the Arızlı region's mineralization potential has been enhanced by utilizing high-resolution geophysical and geochemical methods, highlighting their relevance in analogous global geological contexts. The study may serve as a reference framework for future studies in ophiolitic terrains.

CONCLUSIONS

This study thoroughly assesses the mineralization potential in the Arızlı ophiolitic complex, a significant geological formation in the Afyon region of Turkey. It utilizes an integrated methodology that merges advanced geochemical and geophysical techniques. The findings illustrate the essential interaction among structural controls, lithological differences, and economic mineralization, providing significant insights for academic study and practical exploration endeavours.

The geochemical investigation, performed using XRF and ICP-MS techniques, demonstrated a substantial enrichment of chromium (up to 49.51% Cr_2O_3) and nickel (up to 2145 ppm) in the ultramafic lithologies, which are rock formations with a high magnesium and iron content, especially within dunitic zones. The mineralogical composition, as determined by XRD analysis, revealed the predominance of chromite, serpentine, and magnetite, with elevated Cr/Fe ratios indicating substantial economic potential. These results align with global counterparts, including the Bushveld Complex in South Africa and the Pindos Ophiolite in Greece, underscoring the importance of ultramafic complexes as key targets for strategic mineral exploration.

High-resolution drone-based magnetic surveys identified specific anomalies associated with the ultramafic strata containing chromite and nickel mineralization. Depth slices of 50 m, 100 m, 150 m, and 250 m accurately delineated subsurface lithological and structural characteristics, encompassing fault zones and brecciated serpentinites linked to metal deposits. The resistivity and chargeability data from IP/ERT profiles provide supplementary insights, highlighting underlying ore zones and structural constraints, including faults and lithological boundaries. Integrating drone-based geophysics with ground-based geochemical approaches proved crucial for enhancing the accuracy and reliability of the exploration model.

The results underscore the study's global relevance, highlighting the crucial influence of structural characteristics, including faults and lithological connections, on the control of mineralization. The discontinuities enabled hydrothermal alteration and serpentinization processes, which subsequently concentrated chromite and nickel ores in particular zones. The brecciated and altered zones associated with these formations are promising prospects for further exploration and resource assessment. The study's scientific approach validates the economic potential of the Arızlı complex and establishes a precedent for research tactics in analogous ophiolitic terrains worldwide.

This study acknowledges constraints, including the unexplored subsurface beyond a 250 m depth, which necessitate the use of advanced geophysical methods, such as gravity surveys or seismic imaging. Furthermore, forthcoming metallurgical investigations are required to evaluate the viability of mining and processing these minerals. Extending this methodology to more ophiolitic complexes in Turkey, including the Mersin and İspendere ophiolites, may confirm

its broader relevance. The amalgamation of machine learning algorithms with geophysical and geochemical datasets offers a promising opportunity to enhance the accuracy of mineral deposit predictions.

This research elucidates the mineralization processes in the Arızlı ophiolitic complex and establishes a comprehensive, scalable analytical framework for mineral prospecting in ultramafic terrains. The findings enhance our understanding of vital mineral resources and underscore Turkey's potential as a significant player in the global mineral market. This work offers a crucial step forward in merging contemporary technologies and traditional exploratory approaches to address the challenges of modern mineral exploration, inspiring optimism for the industry's future.

ACKNOWLEDGEMENT

This study encompasses the geological and geophysical investigations conducted under license number 3102414, attributed to Yılmaz Soğukçeşme and Bayram Akdoğan. I want to thank Geophysical Engineer Hurşit Canlı and Abdullah Sipahi for their contributions to this work. The author sincerely thanks the two anonymous reviewers for their constructive comments and valuable suggestions, which significantly improved the quality of the manuscript.

REFERENCES

Accomando, F., Bonfante, A., Buonanno, M., Natale, J., Vitale, S., Florio, G. 2023. The drone-borne magnetic survey as the optimal strategy for high-resolution investigations in presence of extremely rough terrains: The case study of the Taverna San Felice quarry dike. *Journal of Applied Geophysics 217*, 105–186.

Ahmed, A.H., Arai, S. 2003. Platinum-group minerals in podiform chromitites of the Oman ophiolite. *The Canadian Mineralogist 41(3)*, 597–616.

Ali, M.A.H., Mewafy, F.M., Qian, W., Alshehri, F., Ahmed, M.S., Saleem, H.A. 2023. Integration of electrical resistivity tomography and induced polarization for characterization and mapping of (Pb-Zn-Ag) sulfide deposits. *Minerals 13(7)*, 986.

Alshareef, S., Hu, X., Wang, J., Liang, Q., Liu, S., Li, Y., Mohamed-Ali, M.A. 2025. Integrated geological and geophysical approaches to map structural controls of chromite deposits associated with ultramafic–mafic complexes of the Ingasana in the southwestern Blue Nile metallogenic province, SE Sudan. *Ore Geology Reviews 177*, 106–441.

Arai, S.H.O.J.I. 1992. Chemistry of chromian spinel in volcanic rocks as a potential guide to magma chemistry. *Mineralogical Magazine 56(383),* 173–184.

Arai, S., Uesugi, J., Ahmed, A.H. 2004. Upper crustal podiform chromitite from the northern Oman ophiolite as the stratigraphically shallowest chromitite in ophiolite and its implication for Cr concentration. *Contributions to Mineralogy and Petrology 147*, 145–154.

Arasada, R.C., Rao, G.S., Sahoo, P.R. 2020. Integrated geological and geophysical studies for delineation of laterite covered chromiferous ultramafic bodies around Bhuban, southwestern part of Sukinda ultramafic complex, Odisha. *Ore Geology Reviews 119*, 103–402.

Blakely, R.J. 1996. *Potential theory in gravity and magnetic applications*. Cambridge University Press.

Çiftçi, Y., Dönmez, C., Parlak, O., Günay, K. 2019. Chromitite deposits of Turkey in Tethyan ophiolites. In: Pirajno, F., Ünlü, T., Dönmez, C., Şahin, M.B., (eds), *Mineral Resources of Turkey*. Modern approaches in solid earth sciences, v. 16: Cham, Switzerland, Springer, 73–157.

Cox, L.H., Zhdanov, M.S., Pitcher, D.H., Niemi, J. 2023. Three-dimensional inversion of induced polarization effects in airborne time domain electromagnetic data using the GEMTIP model. *Minerals 13(6)*, 779.

Cross, B., Peterson, H. 2023. A comparison of airborne geophysical data over two magmatic nickel deposits. *The Leading Edge*, *42(4)*, 237–244.

Dadrass Javan, F., Samadzadegan, F., Toosi, A., van der Meijde, M. 2024. Unmanned Aerial Geophysical Remote Sensing: A Systematic Review. *Remote Sensing 17(1),* 110.

Dilek, Y., Furnes, H. 2011. Ophiolite genesis and global tectonics: Geochemical and tectonic fingerprinting of ancient oceanic lithosphere. *Bulletin 123(3–4)*, 387–411.

Eskandari, A., Hosseini, M., Nicotra, E. 2023. Application of satellite remote sensing, UAV-geological mapping, and machine learning methods in the exploration of podiform chromite deposits. *Minerals 13(2),* 251.

Fahad, S., Liu, C., Chen, R., Ahmad, J., Yaseen, M., Shah, S. A., El-Kaliouby, H. 2025. Joint Inversion of Audio-Magnetotelluric and Dual-Frequency Induced Polarization Methods for the Exploration of Pb-Zn Ore Body and Alteration Zone in Inner Mongolia, China. *Minerals 15(3)*, 287.

Harris, J.R., Grunsky, E.C. 2015. Predictive lithological mapping of Canada's North using Random Forest classification applied to geophysical and geochemical data. *Computers & geosciences 80,* 9–25.

Işık, V. 2016. *The Geology of the Taurus Mountains.* Turkey Geology Lecture Notes, Ankara University Department of Geological Engineering, *Ankara*. [In Turkish].

Jackisch, R. 2020. Drone-based surveys of mineral deposits. Nature Reviews. *Earth & Environment 1(4),* 187–187.

Jackisch, R., Heincke, B.H., Zimmermann, R., Sørensen, E.V., Pirttijärvi, M., Kirsch, M., Gloaguen, R. 2021. Drone-based magnetic and multispectral surveys to develop a 3D model for mineral exploration at Qullissat, Disko Island, Greenland. *Solid Earth, 13*, 793–825.

Kapsiotis, A.N. 2013. Genesis of chromitites from Korydallos, Pindos Ophiolite Complex, Greece, based on spinel chemistry and PGE-mineralogy. *Journal of Geosciences 58(1),* 49–69.

Kapsiotis, A. 2014. Composition and alteration of Cr-spinels from Milia and Pefki serpentinized mantle peridotites (Pindos Ophiolite Complex, Greece). *Geologica Carpathica 65(1)*, 83.

Kapsiotis, A.N. 2016. Mineralogy, geochemistry and geotectonic significance of harzburgites from the southern Dramala upper mantle suite, Pindos ophiolite complex, NW Greece. *Geological Journal 51(2)*, 236–262.

Kruger, W.A.J. 2021. Massive magnetitite layers of the bushveld complex, South Africa: geology, geochemistry, and genesis. Doctoral dissertation.

Leblanc, M., Nicolas, A. 1992. Ophiolitic chromitites. *International Geology Review 34(7),* 653–686.

Lelièvre, P.G., Farquharson, C.G. 2016. Integrated imaging for mineral exploration. In: Moorkamp M., Lelie`vre P.G., Linde N., Khan A. (eds), *Integrated Imaging of the Earth: Eheory and Applications*. Wiley, 137–166. ISBN 9781118929063.

Li, H., Li, Y., Yang, G., Philemon, L., Wan, Y., Zhao, Q., Wang, P. 2023. Prospecting for ophiolite-type chromite deposit in Sartohay, West Junggar (NW China): Constraints from geological and geophysical data. *Ore Geology Reviews 156*, 105–379.

Li, H., Luo, J., Zhang, J., Li, J., Zhang, Y., Zhang, W., Zhang, M. 2024. Determinants of maximum magnetic anomaly detection distance. *Sensors 24(12)*, 4028.

Maurizot, P., Sevin, B., Lesimple, S., Bailly, L., Iseppi, M., Robineau, B. 2020. Mineral resources and prospectivity of the ultramafic rocks of New Caledonia. *Geological Society, London*, *Memoirs, 51*, 215–245.

Mishra, S.P., Samal, A., Sohel, M., Sethi, K.C., Patnaik, S.K. 2022. The Strategies of Chromite Terrace in Sukinda Valley, India: An Appraisal. *Journal of Scientific Research and Reports 28(12)*, 8–26.

Moezzi Nasab, R., Kamkar-Rouhani, A., Arab-Amiri, A.R. 2023. Development of Drone-Borne Geophysical Surveys for Mineral Exploration. *Journal of Environment and Sustainable Mining 1(2)*, 41–47.

Mokhtari, A.R., Behnia, P., Lafrance, B., Naghizadeh, M., Simons, J.M., Harris, J. 2025. Mineral prospectivity mapping of orogenic gold mineralization in the Malartic-Val-d'Or Transect area, metal earth project, Canada. *Ore Geology Reviews*, 106–498.

MTA. 2023. *Afyon L25 B4 Sheet at a scale of 1:25,000*. Geological map. Ankara.

Park, S., Choi, Y. 2020. Applications of unmanned aerial vehicles in mining from exploration to reclamation: A review. *Minerals 10(8)*, 663.

Parlak, O., Rızaoğlu, T., Bağcı, U., Karaoğlan, F., Höck, V. 2009. Tectonic significance of the geochemistry and petrology of ophiolites in southeast Anatolia, Turkey. *Tectonophysics 473(1–2),* 173–187.

Rashid, M.U., Ahmed, W., Waseem, M., Zamin, B., Ahmad, M., Sabri, M.M.S. 2022. Metallic-Mineral Prospecting Using Integrated Geophysical and Geochemical Techniques: A Case Study from the Bela Ophiolitic Complex, Baluchistan, Pakistan. *Minerals 12(7)*, 825.

Rattenbury, M.S., Cox, S.C., Edbrooke, S.W., Martin, A.P. 2016. Integrating airborne geophysical data into new geological maps of New Zealand mineral provinces. Mineral deposits of New Zealand: exploration and research. *Monograph series (Australasian Institute of Mining and Metallurgy) 31*, 37–44. Carlton: Australasian Institute of Mining and Metallurgy.

Robertson, A.H. 2002. Overview of the genesis and emplacement of Mesozoic ophiolites in the Eastern Mediterranean Tethyan region. *Lithos 65(1–2),* 1–67.

Robinson, P.T., Trumbull, R.B., Schmitt, A., Yang, J.S., Li, J.W., Zhou, M.F., Xiong, F. 2015. The origin and significance of crustal minerals in ophiolitic chromitites and peridotites. *Gondwana Research 27(2)*, 486–506.

Sanusi, S.O., Josiah, D.I.A., Olaniyan, O., Olayanju, G.M. 2024. Delineation of Potential Gold Mineralization Zones in the Kushaka Schist Belt, Northcentral Nigeria, Using Geochemical, Ground Magnetic, Induced Polarization, and Electrical Resistivity Methods. *Mining, Metallurgy Exploration 41(4)*, 2007–2029.

Siemon, B., Ibs-von Seht, M., Steuer, A., Deus, N., Wiederhold, H. 2020. Airborne electromagnetic, magnetic, and radiometric surveys at the German North Sea coast applied to groundwater and soil investigations. *Remote Sensing 12(10)*, 1629.

Sihoyiya, M. 2023. Cost-effective and novel seismic methods for mineral and coal exploration: Examples from Witwatersrand goldfields and Bushveld Complex. Doctoral dissertation. Johannesburg: University of the Witwatersrand.

Smith, R.S., Naghizadeh, M., Cheraghi, S., Adetunji, A., Vayavur, R., Eshaghi, E., Maris, V. 2023. Geophysical transects in the Abitibi greenstone belt of Canada from the mineral-exploration-oriented Metal Earth project. *The Leading Edge 42(4),* 245–255.

Telford, W.M., Geldart, L.P., Sheriff, R.E. 1990. *Applied geophysics.* Cambridge University Press.

Tobi, A., Essalhi, M., Es-Sabbar, S., Qarqori, K., Bouzekraoui, M., Baha, A.A., El Azmi, D. 2025. Application of High-Resolution Gravity and Magnetic Data for Fe-Mn-Pb Mineralization Prospecting in Jbel Skindis, Eastern High Atlas, Morocco. *Economic and Environmental Geology 58(1)*, 17–31.

Tupaz, C.A.J., Watanabe, Y., Sanematsu, K., Echigo, T. 2020. Mineralogy and geochemistry of the Berong Ni-Co laterite deposit, Palawan, Philippines. *Ore Geology Reviews 125,* 103–686.

Wells, M.A., Ramanaidou, E.R., Quadir, M.Z., Roberts, M., Bourdet, J., Verrall, M. 2022. Morphology, composition and dissolution of chromite in the Goro lateritic nickel deposit, New Caledonia: Insight into ophiolite and laterite genesis. *Ore Geology Reviews 143,* 104–752.

Whitney, D.L., Evans, B.W. 2010. Abbreviations for names of rock-forming minerals. *American Mineralogist 95(1),* 185–187.

Yalçın, C., Karan, A. 2024. Application of geophysical methods in subsurface mapping and mineral exploration: Adiyaman-Besni region, Türkiye. *Journal of Geography and Cartography 7(2),* 10193.

Yalçın, C., Kaya, M. 2025. Mineralogical, petrographical and geochemical characterization of chrysotile in the Arızlı ophiolitic mélange (Afyon-Şuhut, Türkiye). *Niğde Ömer Halisdemir Üniversitesi Mühendislik Bilimleri Dergisi [Niğde Ömer Halisdemir University (NOHU) Journal of Engineering Sciences] 14(3)*, 1–1. [In Turkish].

Yang, J., Wu, W., Lian, D., Rui, H. 2021. Peridotites, chromitites and diamonds in ophiolites. *Nature Reviews Earth Environment 2(3)*, 198–212.

Zaccarini, F., Economou-Eliopoulos, M., Tsikouras, B., Garuti, G. 2024. Chromite Composition and Platinum-Group Elements Distribution in Tethyan Chromitites of the Mediterranean Basin: An Overview. *Minerals, 14(8)*, 744.

Zhou, M.F., Robinson, P.T., Malpas, J., Li, Z. 1996. Podiform chromitites in the Luobusa ophiolite (southern Tibet): implications for melt-rock interaction and chromite segregation in the upper mantle. *Journal of Petrology 37(1),* 3–21.

Dossey, M. 2023. PGE Geochemistry and Mineralogy of Dunite, Chromitite, and Laterite Samples from the Acoje Ophiolite Block, Philippines (Dissertation). Retrieved from https://urn.kb.se/resolve?urn=urn:nbn:se:ltu:diva-95281.

Efrem, R., Coutu, A., Saeedi, S. 2024. Sensor Integration and Performance Optimizations for Mineral Exploration using Large-scale Hybrid Multirotor UAVs. arXiv preprint arXiv:2402.11797. https://arxiv.org/abs/2402.11797.